Absolute polarimetry at RHIC

H. Okada[1,*], I. Alekseev[†], A. Bravar[2,**], G. Bunce[**,‡], S. Dhawan[§], K.O. Eyser[3,¶], R. Gill[**], W. Haeberli[‖], H. Huang[**], O. Jinnouchi[4,‡], Y. Makdisi[**], I. Nakagawa[††], A. Nass[5,**], N. Saito[6,*], E. Stephenson[‡‡], D. Sviridia[†], T. Wise[‖], J. Wood [**] and A. Zelenski[**]

[*]*Kyoto University, Sakyo-ku, Kyoto 606-8502, Japan*
[†]*Institute for Theoretical and Experimental Physics (ITEP), 117259 Moscow, Russia*
[**]*Brookhaven National Laboratory, Upton, NY 11973, USA*
[‡]*RIKEN BNL Research Center, Upton, NY 11973, USA*
[§]*Yale University, New Haven, CT 06520, USA*
[¶]*University of California, Riverside, CA 92521, USA*
[‖]*University of Wisconsin, Madison, WI 53706, USA*
[††]*RIKEN, Wako, JAPAN*
[‡‡]*Indiana University Cyclotron Facility, Bloomington, IN 47408, USA*

Abstract. Precise and absolute beam polarization measurements are critical for the RHIC spin physics program. Because all experimental spin-dependent results are normalized by beam polarization, the normalization uncertainty contributes directly to final physics uncertainties. We aimed to perform the beam polarization measurement to an accuracy of $\Delta P_{beam}/P_{beam} < 5\%$.

The absolute polarimeter consists of Polarized Atomic Hydrogen Gas Jet Target and left-right pairs of silicon strip detectors and was installed in the RHIC-ring in 2004. This system features *proton-proton* elastic scattering in the Coulomb nuclear interference (CNI) region. Precise measurements of the analyzing power A_N of this process has allowed us to achieve $\Delta P_{beam}/P_{beam} = 4.2\%$ in 2005 for the first long spin-physics run.

In this report, we describe the entire set up and performance of the system. The procedure of beam polarization measurement and analysis results from 2004 – 2005 are described. Physics topics of A_N in the CNI region (four-momentum transfer squared $0.001 < -t < 0.032$ $(\mathrm{GeV}/c)^2$) are also discussed. We point out the current issues and expected optimum accuracy in 2006 and the future.

Keywords: Elastic scattering, spin, coulomb nuclear interference
PACS: 13.88.+e, 13.85.Dz, 29.27.Pj, 29.27.Hj

Introduction

The RHIC spin physics program has been a unique opportunity and important component of the overall RHIC physics program. Essential to this spin program are the polarized proton beams to investigate spin-dependent structure in the nucleon. Several types of spin-dependent asymmetries in high energy *proton-proton* (*pp*) collisions pro-

---

[1] Present address: Brookhaven National Laboratory, Upton, NY 11973, USA
[2] Present address: University of Geneva , 1205 Geneva, Switzerland
[3] Present address: Deutsches Elektronen Synchrotron, 22607 Hamburg, Germany
[4] Present address: KEK, Tukuba, Japan
[5] Present address: University of Erlangen, 91058 Erlangen, Germany
[6] Present address: KEK, Tukuba, Japan

vide detailed studies of the structure of the proton at a new level of accuracy. Because all experimental results are normalized by beam polarization, P_{beam}, the normalization uncertainty contributes directly to final physics uncertainties. Therefore accurate and absolute polarization measurements are crucial. P_{beam} is obtained from raw asymmetry, ε_{beam}, for the transversely polarized proton beam divided by analyzing power, A_N, of a certain interaction as shown in Equation 1.

$$P_{beam} = \frac{\varepsilon_{beam}}{A_N} \tag{1}$$

We aimed to achieve an accuracy of $\Delta P_{beam}/P_{beam} < 5\%$ at any beam energy from injection (24 GeV/c) to flat-top (100 GeV/c and 250 GeV/c in the near future). Ideal interactions for polarimetry should satisfy the following conditions:

1. well-known or measureable and non-zero analyzing power,
2. high event rate interaction (large cross-section and/or thicker target) to save data taking time,
3. similar kinematics for different beam momenta for common detector set up.

The elastic scattering of the polarized proton beam off a nuclear target A ($p^{\uparrow}A \rightarrow pA$) in the Coulomb nuclear interference (CNI) region is an ideal process. We choose proton and carbon for A. A_N is a function of four-momentum transfer squared, $-t$. We are looking at very small $-t$ in the order of 10^{-3} (GeV/c)$^{-2}$. We have two types of polarimeters to meet above requirements. One is the RHIC pC-polarimeter, which satisfies item 2 and 3. This polarimeter serves as a semi-on-line beam polarization monitor during the RHIC-run period to tune up the beam acceleration. The RHIC pC polarimeter also provides fill-by-fill offline P_{beam} results to experimental groups. However, its accuracy is limited ($\Delta P_{beam}/P_{beam} > 20\%$) mainly due to a difficulty of $-t$ range measurement in pC elastic scattering. This difficulty is connected to the need to caliblate each year. The other polarimeter, the **Polarized Atomic Hydrogen Jet Target Polarimeter** (H-Jet polarimeter in short) serves as an absolute calibration of the RHIC pC polarimeter. The H-Jet polarimeter satisfies item 1 and 3. In this report, we focus on the H-jet polarimeter. Details of the RHIC pC polarimeter are discussed in [1].

The pp elastic scattering process is 2-body exclusive scattering with identical particles. A_N for the target polarization and the beam polarization should be same as shown in Equation 2.

$$A_N = -\frac{\varepsilon_{target}}{P_{target}} = \frac{\varepsilon_{beam}}{P_{beam}}, \tag{2}$$

ε_{target} is *raw* asymmetry for the pp elastic scattering for the transversely polarized proton **target** and P_{target} is a well calibrated polarized proton target, which we will discuss later. Therefore we can change the role of which is polarized between the target proton and the beam proton. Then the beam polarization is measured as:

$$P_{beam} = -P_{target}\frac{\varepsilon_{beam}}{\varepsilon_{target}}. \tag{3}$$

The beauty of the H-Jet polarimeter is that we can cancel the common factors of systematic uncertainty of ε_{target} and ε_{beam}. By accumulating enough statistics, $\Delta P_{beam}/P_{beam} \approx \Delta P_{target}/P_{target}$ is realizable. Although A_N does not appear explicitly in Equation 3, precise measurements of A_N are very important to confirm that the H-Jet polarimeter works properly at any time.

In addition to polarimetry, precise measurements of A_N in the CNI region are important to understand the reaction mechanism completely. The *pp* elastic scattering is described in spin-flip and non-flip transition amplitudes. Each amplitude is a sum of the electro magnetic and hadronic forces as functions of $\sqrt{s}$ and $-t$. A_N is expressed as,

$$A_N \approx -\frac{\mathrm{Im}[\phi^{em}_{SF}(s,t)\phi^{had*}_{NF}(s,t)+\phi^{had}_{SF}(s,t)\phi^{em}_{NF}(s,t)]}{|\phi^{em}_{NF}(s,t)+\phi^{had}_{NF}(s,t)|^2}. \quad (4)$$

The electro magnetic part of amplitudes ($\phi^{em}_{NF}(s,t)$ and $\phi^{em}_{SF}(s,t)$) are precisely understood by quantum electrodynamics (QED). The hadronic part of the non-flip amplitude ($\phi^{had}_{NF}(s,t)$) , which is related to the unpolarized differential cross-section and total cross-section via the optical theorem at $-t = 0$, is also understood very well. The first term of Equation 4 is calculable and has a peak around $-t \simeq 0.003\ (\mathrm{GeV}/c)^2$ [2] which is generated by proton's anomalous magnetic moment.

However, the second term, which includes $\phi^{had}_{SF}(s,t)$, is not well-known. The hadronic reaction in the CNI region is described by non-perturbative quantum chromodynamics (QCD) and a precise prediction is not available. The presence of $\phi^{had}_{SF}(s,t)$ should introduce a deviation in magnitude from the first term and, consequently, there is no precise prediction of A_N. An initial measurement of A_N in the CNI region was performed by the E704 experiment at 200 GeV/c [3]. However, precision of data was insufficient for polarimetry.

In the following sections, we will introduce the H-Jet target system, experimental set up and analysis procedures and then we will report on A_N results from RUN4. We will also report on P_{beam} from RUN5 which was the first long spin-physics run. Finally, we will discuss current issues and expected optimum precision in 2006 and the future.

H-Jet-target system

The system was installed in the RHIC-ring tunnel for the first time in March 2004. The commissioning was successfully done. Assembly sequence of the system had been completed within 15 months [4, 5]. The H-Jet-target system is 3.5 m in height and approximately 3000 kg in weight. The target is a free atomic beam, comes from the top in Figure 1, and crosses the RHIC proton beams perpendicularly. In this report, we define the negative y-axis as the atomic beam direction and the positive z-axis is the RHIC proton beam direction. The velocity of the atomic beam is 1560 ± 20 m/s [4] and negligible with respect to the RHIC beam. The H-Jet-target system is placed on rails along the x-axis. The entire system can be moved along the x-axis by $\pm$10 mm, in order to adjust the target center to the RHIC beam center. As Figure 1 displays, the system consists of mainly 3 parts including nine vacuum chambers and nine differential vacuum stages:

1. Atomic Beam Source, ABS: 1st to 5th chambers. Polarize the atomic hydrogen.
2. Scattering chamber: 6th chamber. Collisions between the target-proton and the beam-proton occur here. The recoil spectrometers are mounted on both sides of flanges.
3. Breit-Rabi Polarimeter, BRP: 7th to 9th chamber. Measure nuclear polarization, $P_{\pm}$.

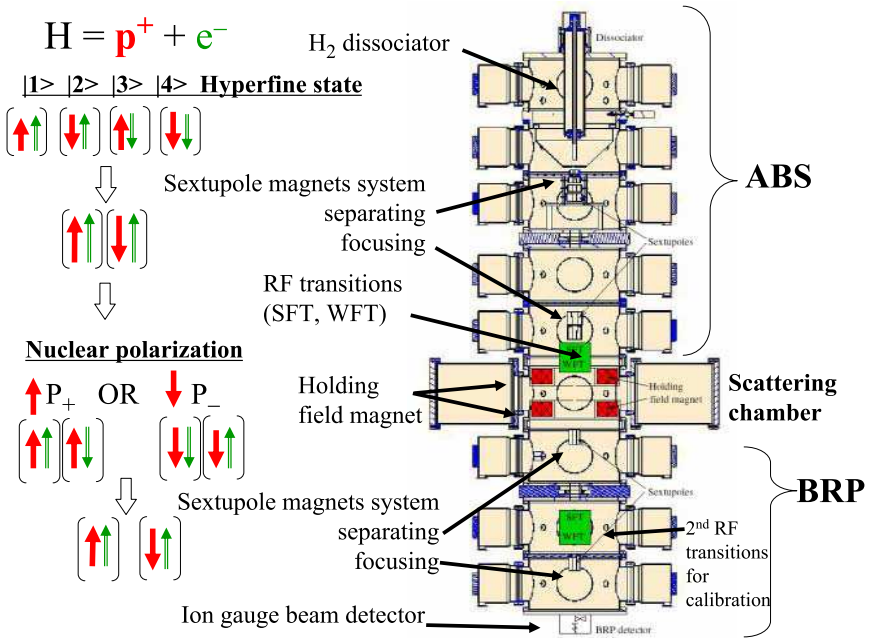

FIGURE 1. H-Jet system overview.

The polarization cycle was $(+/0/-)$=$(500/50/500)$ seconds and Figure 2 displays a sample of the measured $P_{\pm}$ in the 2004 commissioning run [6]. H-Jet-target system was stable over the experimental period. The mean values for nuclear polarization of the atoms:$|P_{\pm}| = 0.958 \pm 0.001$.

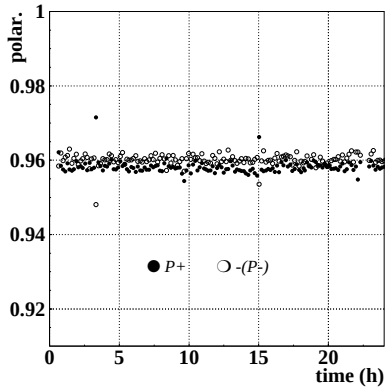

FIGURE 2. Nuclear polarization measured by BRP in 2004.

The BRP measures the atomic hydrogen polarization, therefore we need to account for the effect on the polarization from background hydrogen molecules. Actually, there were still some molecular hydrogen in the scattering chamber and the measurement was $H_2/H \sim 0.015$ [4]. This means that the dilution is about 3% in terms of hydrogen atoms. Assuming the molecular hydrogen is unpolarized, the effective target polarization in the 2004 commissioning run was $P_{target} = 0.924 \pm 0.018$.

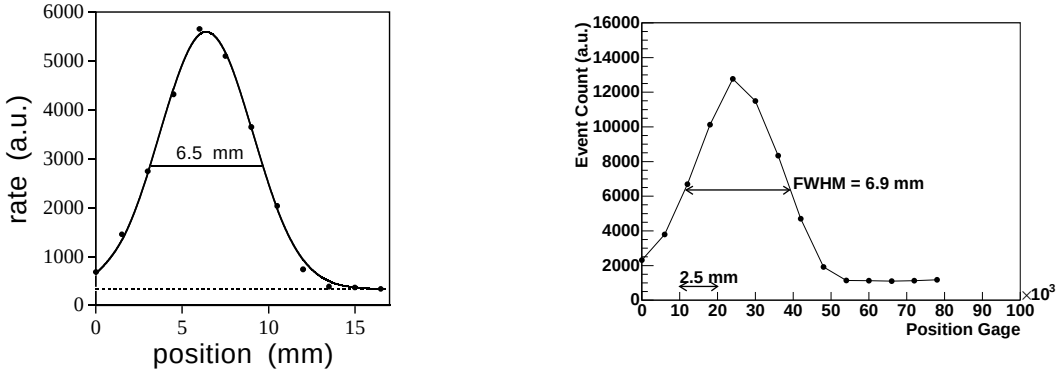

FIGURE 3. Left: Atomic beam profile measurements by the compression tube method. Right: Atomic beam profile measurements by RHIC-beam and the recoil spectrometer.

Next, we describe the profile and the density of atomic beam briefly. The atomic beam profile was measured with a 2mm diameter compression tube. The results are displayed in left side of Figure 3. At the center of the scattering chamber, the FWHM of the atomic beam is 6.5mm and agrees with the design value. Furthermore, we measured the target profile by fixing the RHIC beam ($\sigma \sim 1$ mm) position and moving the entire H-Jet-target system in 1.5 mm steps. The right side of Figure 3 displays event counts detected by recoil spectrometer versus position. Comparing left and right plots of Figure 3, the two independent measurements agree very well. The target profile measurement using RHIC-beam is important to find the best collision point and estimate the unpolarized background fraction. The total atomic beam intensity in the scattering chamber was measured to be $(12.4 \pm 0.2) \cdot 10^{16}$ atoms/s [6]. Taking the measured atomic beam intensity, velocity and profile, the areal target thickness along RHIC beam axis (the z-axis) was calculated to be $(1.3 \pm 0.2) \cdot 10^{12}$atoms$/$cm^2 [4].

Recoil spectrometer

The left side of Figure 4 displays a schematic layout of the experimental set up to detect *pp* elastic scattering events. Recoil protons were detected using an array of silicon detectors located to the left and right of the beam at a distance $D \simeq 80$ cm. Three pairs of silicon detectors covered an azimuthal angle of 15° centered on the horizontal mid-plane. Detectors were 70.4×50 mm^2 in size, with a 4.4 mm read out pitch for a total of 16 channels per detector. We cover recoil protons of kinetic energy of $0.6 \leq T_R \leq 17.0$ MeV. The recoil angle, θ_R, is obtained by the detector channel number in $\simeq$ 5.5 mrad steps. This angular resolution is comparable to the H-Jet-target size.

The silicon detectors were ~ 400 μm thick. Recoil protons with kinetic energies,T_R, up to 7 MeV are fully absorbed. The energy calibration of the silicon detectors was performed using two α sources ^{241}Am, 5.486 MeV (and ^{148}Gd, 3.183 MeV for three out of six detectors). Resolution of T_R in the fully absorbed region is $\Delta T_R = 0.6$ MeV. More energetic protons punched through the detectors, depositing only a fraction of their energy. Therefore T_R for punch-through protons needs to be corrected using the detector thickness and tables for energy loss in silicon [7]. The 4-momentum transfer

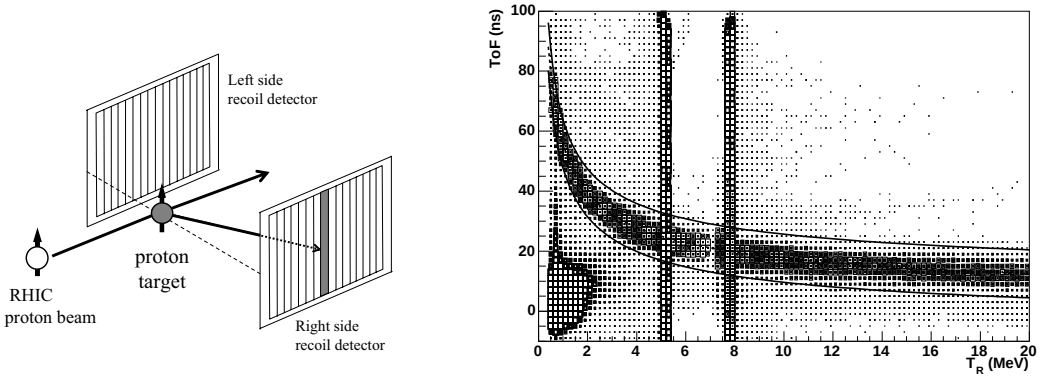

FIGURE 4. Left:Sketch of left-right pair of silicon detectors. Right: The correlation between TOF and the incident energy, T_R, in one of the silicon detectors. Two solid lines corresponds to ± 8 nsec shifted with respect to the expected TOF value for given T_R from Equation 5.

squared is given by $-t = 2M_pT_R$. The time-of-flight, TOF, is measured with respect to the bunch crossing timed by the accelerator RF clock. The estimated TOF resolution is $\Delta\text{TOF} \simeq 3$ nsec and a result of the intrinsic time resolution of the detectors (≤ 2 nsec) and the length of the RHIC beam bunches ($\sigma \simeq 1.5$ nsec). Details of the recoil spectrometer and analysis for RUN4 are discussed in [8].

Elastic event selection

In the *pp* elastic scattering process, both the forward-scattered particle and the recoil particle are protons and no other particles are produced in the process. The elastic process can be identified by detecting the recoil particle only, by identifying the recoil particle as a proton throughout the relation of TOF and T_R, and by observing that the missing mass of the forward scattered system is the proton mass. Recoil protons were identified using the non-relativistic relation

$$T_R = \frac{1}{2}M_p(D/\text{TOF})^2. \tag{5}$$

The right plot of Figure 4 displays T_R and TOF correlation from one detector for 16 channels. We can see recoil protons clearly around the expected TOF value for T_R. In this figure, the energy for punch-through events have been corrected [8, 9]. The events which are vertically distributed around 5.5 MeV are from the calibration α source (^{241}Am). (The punch-through correction causes another vertical distribution around 7.5 MeV.) Events less than 3 MeV and less than 30 nsec are prompt particles, which are possibly pions from beam-related interactions upstream. Events were selected in a TOF interval of ± 8 nsec around the expected TOF value for recoil protons of a given T_R as shown in two lines in the figure.

On the basis of the measured θ_R and T_R, the mass of the undetected forward scattered system (the missing mass M_X) can be reconstructed,

$$M_X{}^2 = M_p{}^2 - 2\Big((M_p + E_1)T_R - \sin\theta_R\sqrt{2M_pT_R(E_1^2 - M_p^2)}\Big), \tag{6}$$

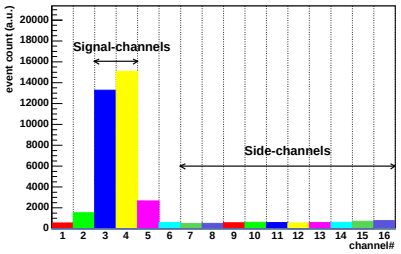

FIGURE 5. Event distribution of a certain T_R interval as function of channel number.

where E_1 is the energy of the incident beam proton. For pp elastic scattering, events are identified on the basis of the θ_R-T_R relation

$$T_R = 2M_p \sin^2\theta_R \frac{E_1 - M_p}{E_1 + M_p}, \tag{7}$$

which is obtained applying $M_X = M_p$ in Equation 6. The difference for $E_1 = 24$ GeV and $E_1 = 100$ GeV, the two beam energies reported here, is ~ 3 mrad at $T_R = 17$ MeV and smaller shift at lower energies Figure 5 displays the event distribution of a certain T_R interval as function of channel number. For each T_R bin pp elastic events were selected in the proper detector strips centered around the expected θ_R angle.

The channel for diffractive dissociation opens at $M_X > M_p + M_\pi = 1.08$ GeV$/c^2$. The kinematical boundary for $M_X = M_p + M_\pi$ is given by Equation 6 and is out of the acceptance for $E_1 = 24$ GeV. For $E_1 = 100$ GeV, the kinematical boundary for the $M_X = M_p + M_\pi$ is inside the acceptance for $T_R > 8$ MeV. But the contamination is estimated to be less than 0.5% from M_X spectra.

The selected event yield is sorted by T_R bins. We collected 4.3 M events in fourteen T_R bins at 100 GeV/c and 0.8 M events in nine T_R bins at 24 GeV/c in the region $0.001 \leq -t \leq 0.035$ (GeV/c)^2 ($0.5 \leq T_R \leq 17$ MeV) using the "clock-wise" beam. Furthermore, the selected event yield in each T_R bin is sorted by spin states (beam, target, up-down) and the detector side (left-right). Finally, we calculate *raw* asymmetries of target or beam polarization using the square-root formula:

$$\varepsilon = \frac{\sqrt{N^L_\uparrow \cdot N^R_\downarrow} - \sqrt{N^R_\uparrow \cdot N^L_\downarrow}}{\sqrt{N^L_\uparrow \cdot N^R_\downarrow} + \sqrt{N^R_\uparrow \cdot N^L_\downarrow}}, \tag{8}$$

where if we sort by H-Jet-target (beam) polarization, we have ε_{target} (ε_{beam}). This expression cancels luminosity and acceptances asymmetries.

A_N measurements from RUN4

A_N data are obtained as follows:

$$A_N = -\frac{\varepsilon_{target}}{P_T} \frac{1}{1 - R_{BG}}, \tag{9}$$

where R_{BG} is the background levels for each T_R bin. The backgrounds consisted of (a) α particles from the calibration sources, (b) beam scraping, and (c) beam scattering from

the unpolarized residual target gas. The dominant component was (c), due to unfocused molecular hydrogen, and was accounted for as a dilution of the target polarization. Therefore, R_{BG} is estimated to be $0.02 \sim 0.03$ from (a) and (b) [9].

Figure 6 displays the results for A_N at 100 GeV/c (open circles) and 24 GeV/c (black filled circles) in 2004. The uncertainties shown are statistical. The lower bands represent the total systematic uncertainties. The thick and thin solid lines are the QED prediction with no spin-dependent hadronic contribution (ϕ_{SF}^{had}) and corresponds to the first term in Equation 4 at these beam momenta.

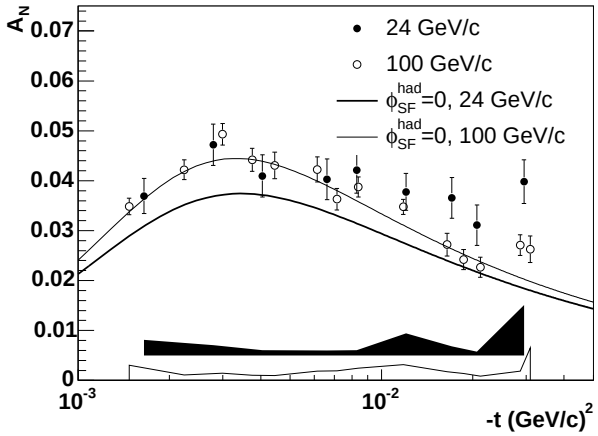

FIGURE 6. A_N data at 24 GeV/c and 100 GeV/c. The uncertainties shown are statistical and lower bands represent the systematic ones. Thick and thin solid lines are the QED prediction without ϕ_{SF}^{had}.

Sources of systematic uncertainties come from T_R bin-dependent and overall normalization: (1) the uncertainty on the target polarization giving an overall $\Delta P_{target}/P_{target} =$ 2.0% normalization uncertainty; (2) the left-right detector acceptance asymmetry; (3) event selection criteria; and (4) background contribution from (a) and (b). The major component was (2) at the lowest and highest T_R bins from detector edges. We also have a relatively large acceptance asymmetry at the punched-through energy region.

For the A_N measurements, we averaged beam spin up-down states to obtain unpolarized beam. The difference of absolute value of beam polarization between spin-up and spin-down states was confirmed to be small by acquiring the results from the RHIC-pC polarimeter. Therefore the residual components beam polarization has no effect on this result.

The A_N data at 24 GeV/c ($\sqrt{s} = 6.8$ GeV) and 100 GeV/c ($\sqrt{s} = 13.7$ GeV) are consistent in the region of $-t < 10^{-2}$. However, these A_N results at different $\sqrt{s}$ energies indicate a $\sqrt{s}$ dependence of $\phi_{SF}^{had}(s,t)$. The A_N data at $\sqrt{s} = 6.8$ GeV are *not* consistent with the solid line (χ^2/ndf=35.5/9) and this discrepancy implies the presence of a hadronic spin-flip contribution, $\phi_{SF}^{had}(s,t)$ [10]. On the other hand, the A_N data at $\sqrt{s} =$ 13.7 GeV are consistent with the QED prediction (χ^2/ndf=13.4/14) [9].

The theoretical efforts to determine $\phi_{SF}^{had}(s,t)$ including its $\sqrt{s}$ dependence are ongoing. Using experimental results (A_N in pp elastic scattering at $\sqrt{s} = 13.7$ GeV and in pC elastic scattering at $\sqrt{s} = 6.4$ GeV [11] and 13.7 GeV [12]) as input parameters, prediction for A_N at $\sqrt{s} = 6.8$ GeV was given in recent work [13]. The prediction suggested a significant $\sqrt{s}$ dependence of $\phi_{SF}^{had}(s,t)$, and agreed with our data within 1-σ uncer-

tainty. More comparisons between theoretical prediction and further experimental data at different beam momenta are required to understand $\phi_{SF}^{had}(s,t)$.

P_{beam} results from RUN5

In 2005, one of the two RHIC beams was centered on the H-Jet-target for several days to accumulate enough statistics for a precise measurement of the beam polarization. We displaced the "unused" beam approximately 10 mm horizontally and vertically from the H-Jet-target center. Both beams were measured repeatedly over the course of a few weeks. Detailed experimental set up and analysis for RUN5 are discussed in [14]. We accumulated 5.3 M events for the "clock-wise" beam and 4.2 M events for the "counter-clock-wise" beam. ε_{target} and ε_{beam} for both beams were calculated using Equation 8. We confirmed that $A_N = -\varepsilon_{target}/P_{target}$ from both beams were consistent with A_N of 2004 results. For polarimetry use, we use data in the peak asymmetry region of $1 \leq T_R \leq 4$ MeV to eliminate acceptance asymmetry and prompt events. Then, P_{beam} is obtained using Equation 3. The total systematic uncertainty in 2005 was $\Delta P_{target}^{sys.}/P_{target} = 2.9\%$. The dominant two components were:

- backgrounds from residual gas and displaced (not used) beam (2.2%),
- uncertainty on the target polarization giving an overall $\Delta P_{target}/P_{target} = 2.0\%$.

Studies of backgrounds were carried out by varying the measured background contributions near the elastic *pp* signal. The strip distributions show a uniformly spread yield over the non-signal strips. (An example at a certain T_R interval is shown in Figure 5.) By increasing the number of strips used for the elastic peak, the background contribution can be increased in a controlled way. Figures 7 and 8 explain this study of the "clock-wise" beam and the "counter-clock-wise" beam. The right parts of these figures summarize the asymmetry ratios for different number of strips for the signal region, going from one to eight. The original asymmetries were calculated with two strips. The open circle and open diamond symbols on the left refer to four and eight strips, thereby doubling and quadrupling the background contributions. Asymmetry ratio of the "clock-wise" beam seems to drop slightly, and that of the "counter-clock-wise" beam rises, but the variations are smaller than the statistical uncertainties. Therefore, these differences do not necessarily point to a polarization dependence of inelastic events. Also, no clear asymmetry has been seen in background events. Absolute beam polarizations of the "clock-wise" and the "counter-clock-wise" beams at 100 GeV/c in 2005 are $49.3\% \pm 1.5\%(\text{stat.}) \pm 1.4\%(\text{sys.})$ and $44.3\% \pm 1.3\%(\text{stat.}) \pm 1.3\%(\text{sys.})$. We achieved accurate beam polarization measurement $\Delta P_{beam}/P_{beam} = 4.2\%$.

Future prospect

Finally, the current issues and expected optimum precision in 2006 and the future are discussed here briefly. More data are collected in RUN6, 8.2 M events for the "clock-wise" beam and 10.7 M events for the "counter-clock-wise" beam at 100 GeV/c. The expected statistical uncertainty is approximately 1 %. More detailed study of background contribution to systematic contribution is ongoing. An improvement to reduce the uncertainty for the unpolarized fraction of the H-Jet-target is required for a breakthrough to a new level of accuracy.

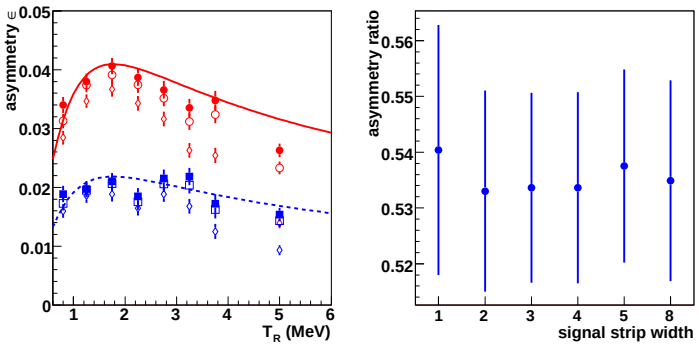

FIGURE 7. Background study for the "clock-wise" beam of RUN5. Left: Filled circle refers to two strips for the original asymmetry. Open circle and open diamond symbols refer to four and eight strips. Upper group is ε_{target} and lower group is ε_{beam}. Right: Asymmetry ratio as a function of signal strip width.

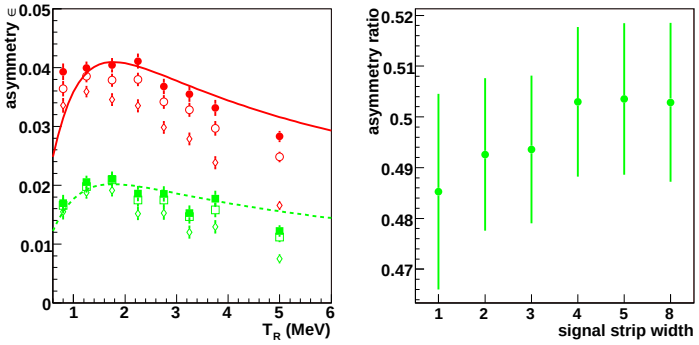

FIGURE 8. Same as Figure 7 for the "counter-clock-wise" beam of RUN5.

A_N data at different beam energies are an important physics topic. In RUN6, we also took 31 GeV/c data with better statistics than RUN4 24 GeV/c. These data will contribute to a comprehensive understanding of $\phi_{SF}^{had}(s,t)$.

REFERENCES

1. I. Nakagawa *et al.*, these proceedings.
2. N.H. Buttimore *et al.*, Phys. Rev. D **59**, 114010 (1999).
3. N. Akchurin *et al.*, Phys. Rev. D **48**, 3026 (1993).
4. T. Wise, A. Zelenski and A. Nass *et al.*, Proc. 16th International Spin Physics Symposium SPIN2004, p. 757, p. 761 and p. 776.
5. Y. Makdisi *et al.*, Proc. 17th International Spin Physics Symposium SPIN2006, p. 975.
6. A. Zelenski *et al.*, Nucl. Inst. and Meth. A **536**, 248 (2005).
7. http://physics.nist.gov/PhysRefData/Star/Text/contents.html
8. H. Okada, Doctoral thesis, July (2006); http://www.star.bnl.gov∼hiromi/HiromiOkadaThesis.pdf
9. H. Okada *et al.*, Phys. Lett. B **638**, 450 (2006).
10. H. Okada *et al.*, Proc. 17th International Spin Physics Symposium SPIN2006, p. 681.
11. J. Tojo *et al.*, Phys. Rev. Lett. **89**, 052302 (2002).
12. O. Jinnouchi *et al.*, Proc. 16th International Spin Physics Symposium SPIN2004, p. 515.
13. L. Trueman, BNL-HET-07/14, 2007; *hep-ph*/0711.4593 (to be published).
14. K.O. Eyser, Proc. 17th International Spin Physics Symposium SPIN2006, p. 916.